

FIRST RESULTS FROM TEXTOR

H. Soltwisch, H.L. Bay, G. Bertschinger, P. Bogen, H. Conrads, K.H. Dippel, G. Fuchs, H. Gerhauser, B. Giesen, E. Graffmann, E. Hintz, F. Hoenen, A. Kaleck, L. Könen, M. Korten, M. Lochter, N. Noda⁺, A. Pospieszczyk, U. Samm, J. Schlüter, B. Schweer, F. Waelbroeck, G. Waidmann, L.H. Wei⁺⁺, P. Wienhold, J. Winter, G. Wolf

Institut für Plasmaphysik der Kernforschungsanlage Jülich GmbH, Association EURATOM-KFA,
D-5170 Jülich

ABSTRACT

The paper summarizes the main results obtained during the first six months of experimental work on TEXTOR with ohmically heated plasmas. The machine ($R = 175$ cm; $a = 45-50$ cm) was operated at wall temperatures up to 300 °C with hydrogen gas, a toroidal field of 2 T and a maximum plasma current of 500 kA, yielding central electron temperatures of 1.2 keV, maximum line-averaged densities of 4×10^{13} cm⁻³ and discharge durations of up to 2.7 sec (for $I_p \leq 340$ kA). Besides providing long-lasting reproducible plasmas for forthcoming plasma-wall interaction research, the following tasks were accomplished: (1) control of low Z impurities by effective wall cleaning and conditioning; (2) accurate plasma positioning for extended pulse durations; (3) determination of the current density distribution by way of Faraday rotation measurements; (4) investigation of plasma limiter interaction including spectroscopic determination of released neutral particle fluxes and measurement of the power density distribution in the scrape-off layer by infrared-thermography.

KEYWORDS

Tokamak performance, plasma position control, wall cleaning and conditioning, impurities, scrape-off layer, current density distribution, Faraday rotation, infrared-thermography.

1. INTRODUCTION

TEXTOR - a medium size "Tokamak Experiment for Technology Oriented Research" - has been constructed primarily to investigate the various and largely interdependent processes which make up the complex field of plasma wall interaction (Conrads, 1978). This scope not only includes a detailed analysis of particle and energy exchange between the plasma and the surrounding chamber but also involves active measures to optimize the first wall and the plasma boundary region in such a way that wall erosion, particle release, and impurity influx to the plasma core are reduced to tolerable levels. In order to comply with these objectives TEXTOR has a number of special design features, such as

- excellent access for diagnostics to domains near to the wall,
- large portholes suitable for implementing methods to control the plasma boundary,
- facilities to heat the vacuum vessel (< 300 °C) and the liner (≤ 600 °C),
- provisions for fast exchange of the liner (by splitting the machine into two parts).

Evidently, a prerequisite for relevant plasma-wall interaction research is a sufficiently hot and dense plasma which can be maintained long enough to bring about stationary conditions with regard to wall temperature, gas recycling, etc. Therefore the capability for long duration discharges is another important characteristic of TEXTOR.

After completion of the technical commissioning in January 1983 the first six months of experimental work were mainly devoted to the generation and control of reproducible long-pulse plasmas with ohmic heating. Besides exploring the accessible range of plasma parameters and testing various diagnostic systems under machine conditions, the efforts concentrated upon the following issues:

⁺ permanent address: Institute of Plasma Physics, University of Nagoya, Nagoya, Japan
⁺⁺ on leave of absence from Institute of Plasma Physics, Academia Sinica, Heifei, People's Republic of China

- (1) Cleaning and conditioning of the liner and of the limiters by different techniques in order to reduce substantially the release of low Z impurities and to control the hydrogen recycling; in situ measurement of the recycling constant for different wall conditions.
- (2) Tokamak operation in a broad range of liner temperatures (between 20 °C and 300 °C).
- (3) Accurate positioning of the plasma inside the limiter aperture including pre-programmable rapid displacements during a discharge.
- (4) Determination of poloidal magnetic field distributions and current density profiles by Faraday rotation measurements using a multi-channel far-infrared interferometer/polarimeter.
- (5) Spectroscopic evaluation of neutral hydrogen and metal impurity fluxes emitted from the limiters and of the impurity concentrations in the plasma core.
- (6) Measurement of the temperature distribution on the limiter surface by infrared-thermography to determine the energy flux and to characterize the scrape-off layer.

This paper summarizes the main results of these investigations starting with a brief presentation of the Tokamak performance and the plasma properties of TEXTOR.

2. PERFORMANCE

For the majority of discharges the machine was operated with hydrogen gas, a toroidal field of 2 T and a maximum plasma current of 330 kA, yielding pulse lengths of up to 2.7 sec. The four poloidal limiters (Inconel 600, later replaced by stainless steel) were usually set at a radius of 45-50 cm. Typical waveforms for loop voltage U_L , plasma current I_p , line-averaged electron density \bar{N}_e and central electron temperature T_{e0} are shown in Fig. 1a. For this particular discharge - as for most of the run time during the first experimental phase - the vacuum vessel was heated to 150 °C and the liner to 300 °C. It was found that after proper conditioning of the liner (cf. chapter 3) its temperature had practically no effect on the Tokamak performance (at least within the explored range from 20 °C to 300 °C).

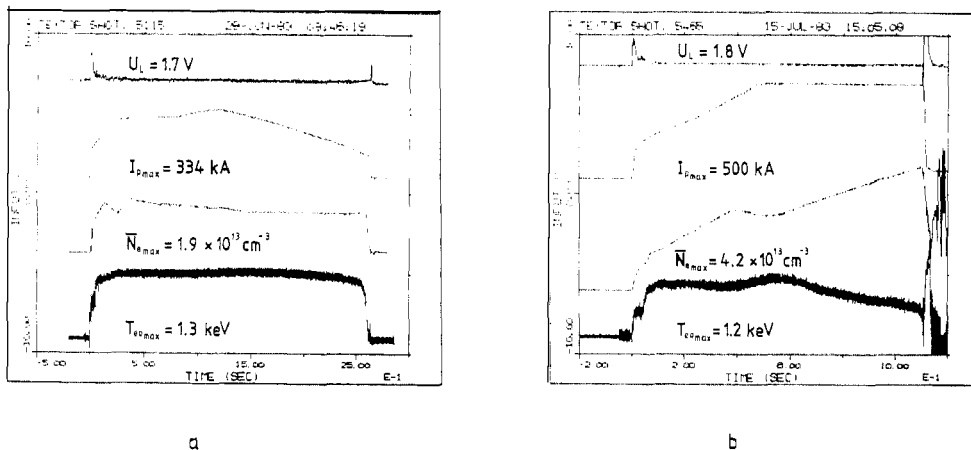


Fig. 1. Waveforms of loop voltage (U_L), plasma current (I_p), line-averaged density (\bar{N}_e) and central electron temperature (T_{e0}) for (a) a representative 300 kA discharge, and (b) a 500 kA discharge with additional gas injection at constant rate during the current flat-top time.

Recently, the plasma current was increased to its lay-out value of 500 kA (corresponding to a safety factor of $q(a) = 2.3$ with $a = 45$ cm) and kept at this level for more than 600 msec. Fig. 1b gives an example of such a discharge with additional gas injection at constant rate during the current flat-top time. The discharge was terminated by a violent disruption when the line-averaged density reached a value of $4.2 \times 10^{13} \text{ cm}^{-3}$. This limit is in agreement with an empirical scaling law derived by Equipe TFR (1980) if Z_{eff} is taken to be 1.2. By properly shutting off the gas feed and ramping down the current, severe disruptions were prevented and the plasmas could be preserved for total durations of up to 2.2 sec.

Table I: TEXTOR Performance data

Plasma current (kA)	330	500	Rogowski coils
Loop voltage (V)	1.7	1.8	flux loops
safety factor q(a)	4.8 (a=50 cm)	2.3 (a=45 cm)	
Pulse duration (sec)	≤2.7	≤2.2	
Line-averaged electron density (10^{13} cm^{-3})	≤2.1	≤4.2	interferometer (2 mm and 337 μm)
Central electron density (10^{13} cm^{-3})	≤3.0	≤5.5	9-channel interferometer (337 μm)
Central electron temperature (keV)	1.3	1.2	Thomson scattering soft x-ray emission electron cyclotron emission
Central ion temperature (keV)	0.8	0.7	neutral particle analysis
Central current density (Acm^{-2})	200	200	9-channel polarimeter (337 μm)
Central Z_{eff}	1.7	1.7	soft x-ray spectroscopy
Enhancement of resistivity on the magnetic axis	4.4	4.2	
Pooidal beta	0.2	0.2	compensated magnetic loop
Electron energy confinement time (msec) ¹⁾	20	25	¹⁾ calculated from N_e - and T_e -profiles

major radius 175 cm; minor radius 45-50 cm; working gas hydrogen; data referring to 1 sec after start-up

The main characteristics of both the 300 kA discharges and the recent 500 kA shots are summarized in Table 1 together with the diagnostics employed to evaluate the basic plasma parameters. Space and time resolved information on the electron density was obtained from a nine-channel far-infrared interferometer. The 300 kA discharges usually showed almost parabolic profiles with flattened centres ($r/a \lesssim 0.2$), and the 500 kA shots yielded rather broad distributions $\sim [1 - (r/a)^4]$ during the flat-top time with strong gas injection (cf. Fig. 5a). The temporal development of the T_e -profiles was determined - besides by Thomson scattering on a shot to shot basis - by observing the soft x-ray continuum radiation along five different chords and by scanning the electron cyclotron emission along the major radius (Waidmann, this conference) with time resolutions of 500 msec and 100 msec, respectively. In general, the electron temperature was quite sharply peaked on axis even for the 500 kA discharges, whereas the current density distribution (determined from far-infrared polarimetry; cf. chapter 5 and Fig. 5b) showed a flat maximum of about 200 Acm^{-2} corresponding to a safety factor of $q(0) = 0.9$. As a consequence, the plasma resistivity on the magnetic axis was enhanced by a factor of 4 relative to the Spitzer value for a pure hydrogen plasma with a central electron temperature of 1.15 keV. On the other hand, spectroscopic measurements of the impurity concentrations in the plasma centre yielded an effective ion charge of $Z_{\text{eff}}(0) \lesssim 1.7$ (cf. chapter 6). The enhancement of resistivity rapidly decreased towards larger radii.

3. WALL CLEANING AND CONDITIONING

Stainless steel and Inconel, commonly used as wall materials in Tokamak devices, are prone to forming thin but resistant films of oxides, carbides and hydrocarbons on their surface, which can be an abundant source of low Z impurities for the plasma. Wall conditioning is therefore required to remove these layers and to restore clean metallic surfaces. For TEXTOR a method has been developed which utilizes a radiofrequency assisted glow discharge in hydrogen (RG discharge; Waelbroeck et al., 1980). Atomic hydrogen created in this discharge readily reacts with the impurity layer and forms volatile products (H_2O , CH_4 , C_2H_6 , etc.) which can be pumped out of the torus, unless the electron temperature is high enough to cause substantial re-dissociation (the latter is probably the main obstacle to cleaning the walls efficiently by running Tokamak discharges). The technical equipment for producing RG discharges essentially consists of three movable antennas and a combined rf/dc power supply and is fairly simple compared to the microwave instrumentation required for electron cyclotron resonance (ECR) discharges, which act in a similar way and have also been employed in TEXTOR. Moreover the wall is at ground potential, thus permitting arbitrary access to the machine during the cleaning process.

The effectiveness of RG discharges was demonstrated by purposely introducing a known amount of oxygen into the thoroughly pre-cleaned TEXTOR vessel at a liner temperature of 210 °C (Waelbroeck *et al.*, 1983). According to residual gas analysis, 90 % was gettered corresponding to 7.2 equivalent monolayers of oxygen absorbed by the inner liner surface (Inconel 625). Subsequently the total amount could be removed within some 20 minutes. After a major opening of the vacuum vessel, TEXTOR was restored to good operation within a few days by an appropriate combination of baking and RG conditioning.

A sensitive indicator for the wall condition is the hydrogen recycling constant $R_C = \alpha\psi \cdot \tau_R$ where $\alpha\psi$ is the flux density of atomic hydrogen penetrating into the wall and τ_R is the characteristic release time of hydrogen molecules. High values of R_C imply strong absorption of hydrogen during Tokamak discharges (wall pumping), which would be disastrous for the large devices aimed at tritium operation. In TEXTOR the recycling constant of the liner was measured in situ by observing the wall pumping and release effect after start-up or sudden termination of RG discharges (Wienhold *et al.*, this conference). It was found that wall contamination by oxygen raised R_C by two orders of magnitude over the value for a cleaned liner ($\sim 1.5 \times 10^{15} \text{ cm}^{-2}$), whereas a coverage with a thin film of carbidic carbon reduced it by a factor of 10.

By adding ~ 1 % of CH_4 to the working gas of an RG discharge it was expected, in the first place, to further deplete strongly bonded surface oxides (e.g. Cr_2O_3) by the formation of volatile CO molecules and, secondly, to deposit a thin layer of carbidic carbon on the liner and the limiters in order to replace the sputtering of metal atoms during Tokamak discharges partly by that of carbon. A corresponding experiment in TEXTOR (Winter *et al.*, this conference) confirmed the depletion of surface oxides and indicated a reduction of the line radiation from metal impurities and oxygen (O VI) but increased C V radiation. The information obtained so far is, however, still incomplete to permit a final valuation of the benefits of carbidic layers on the first wall.

4. PLASMA POSITION CONTROL

In order to achieve and maintain an accurate position of the plasma relative to the surrounding walls, TEXTOR is equipped with an elaborate pre-programmable and feedback control system for independent adjustments of the plasma current and of the vertical and horizontal plasma position (Gerhauser, 1978; Brocke and Waidmann, 1982). The system also allows defined plasma shifts with a velocity of about 1 cm/msec, which can be used to vary the particle and energy flux on to specific limiter sections during a discharge and, by that means, derive information on the impurity release rates (cf. chapter 6) and on the energy flux and the scrape-off layer (cf. chapter 7). Furthermore, well-defined plasma displacements will be of great importance for forthcoming pump limiter experiments on TEXTOR (Bieger *et al.*, 1976; Conn *et al.*, 1982).

The plasma position, which is required as control signal for the feedback system, is usually defined with respect to the poloidal flux pattern. In TEXTOR the centre of the outermost flux surface is determined by magnetic sensor coils mounted outside the liner. Signals induced by plasma motions are actively integrated and fed into an analogue computer to yield the vertical and horizontal shifts Δv and Δh . A drawback of this technique is its sensitivity to plasma motions rather than to displacements, which makes it difficult to control very slow drifts of the plasma column. For prolonged discharge times these may eventually lead to undetected displacements.

To overcome this problem two alternative methods of position detection were studied using a multi-channel far-infrared interferometer/polarimeter (Soltwisch, 1983). The first approach, following a proposal of Waidmann (1979), was aimed at centering the density profile inside the limiter aperture. Its basic idea was to sense horizontal displacements by measuring the phase difference between two vertical probing beams located symmetrically to the vessel centre ($x/a = \pm 0.6$; see Fig. 2.). The experimental accuracy of phase shift detection ($\lesssim 0.02 \times 2\pi$ during the flat-top time of plasma current) allowed to control the horizontal zero position of the density profile to within a few millimeters for arbitrary discharge durations. The stationary positioning was confirmed by a TV camera system observing either the corona of H_α radiation emitted from the plasma edge or the thermal load on the limiter (by viewing through an infrared filter).

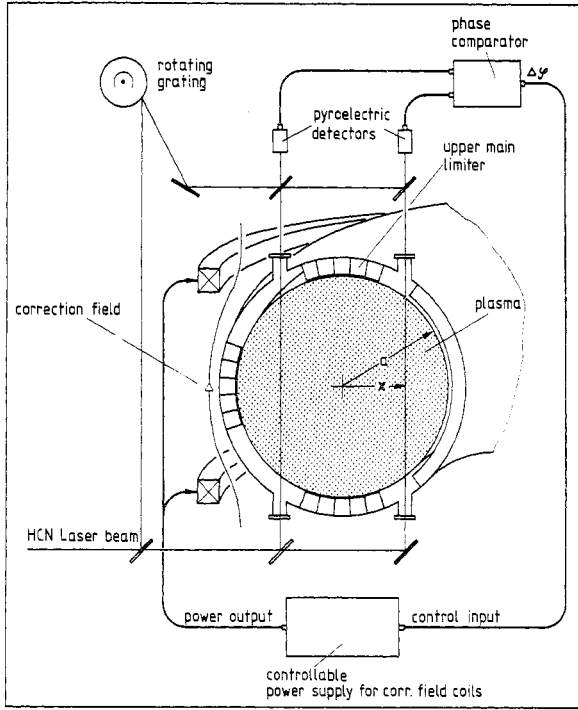


Fig.2 Principle of interferometric plasma position detection

This simple interferometric technique was later improved by normalizing the phase difference to the slope of the phase shift profile as detected by two adjacent probing beams. Thus a direct measure of the horizontal displacement was obtained which made it possible to lock the plasma position on to set values different from zero. Fig. 3a shows an example for a discharge with pre-programmed outward shift of a few cm during the flat-top time. The position signal Δh_m derived from the magnetic diagnostic confirmed this displacement but also indicated some slow motion which was, however, not observed by the TV camera system (the offset in Δh_m is due to an eccentric installation of the sensor coils relative to the plasma zero position).

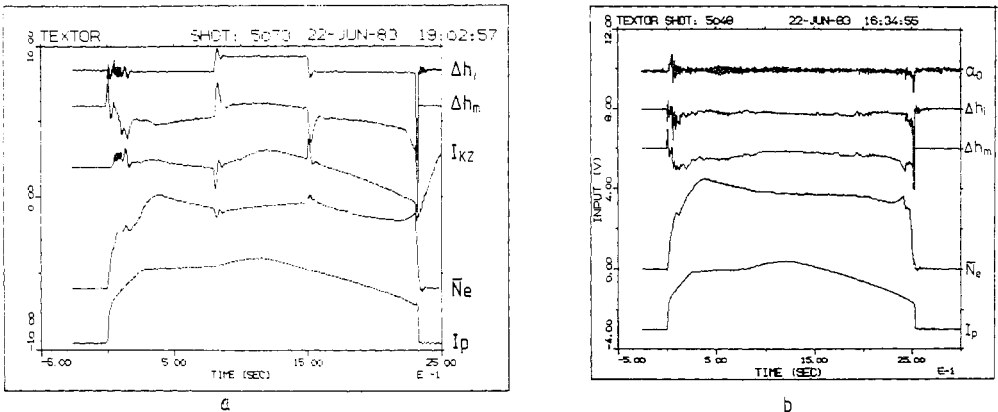


Fig.3 Horizontal position signals ($\Delta h_i, \Delta h_m$), current in the vertical correction field coils (I_{kz}), line-averaged density (N_e) and plasma current (I_p) for (a) a discharge with pre-programmed outward shift controlled by means of the interferometric signal Δh_i , and (b) a discharge controlled by means of the Faraday rotation signal α_0 .

The second approach to position detection made use of the Faraday effect experienced by a linearly polarized probing wave passing vertically through the vessel centre. Only in case of well-centred flux surfaces there would be no parallel magnetic field component along the beam path and hence no Faraday rotation of the plane of polarization. Polarimetric measurements of the rotation angle yielded a resolution of 0.15 deg (limited by detector noise), which was sufficient to fix the horizontal plasma position to about ± 1 cm (Fig. 3b). Both the interferometric and polarimetric technique were employed in several hundred shots under a variety of discharge conditions. The vertical plasma position was thereby detected and controlled by means of the iso-flux method.

5. MEASUREMENT OF THE CURRENT DENSITY DISTRIBUTION

There is as yet no well-established method for measuring the current density distribution (or equivalently the distribution of the poloidal magnetic field) in Tokamak plasmas. On TEXTOR we have tried to derive the current density profile from simultaneous measurements of phase shifts ($\sim \sqrt{N_e} dz$) and Faraday rotation angles ($\sim \sqrt{N_e} B_{\theta} dz$) using a nine-channel HCN laser interferometer/polarimeter (N_e is the electron density and B_{θ} is the poloidal field component parallel to the probing beam; the integrals are taken along the vertical beam paths in the plasma cross section). The general lay-out of the instrument is similar to the multi-channel interferometer on the TFR Tokamak (Veron *et al.*, 1977) with some additions for simultaneous Faraday rotation measurements (Soltwisch and Equipe TFR, 1981). The number of channels and their distribution across the plasma (cf. Figs. 4a,c) are sufficient to allow Abel inversion of the experimental data and thereby evaluate the electron density profile and the poloidal magnetic field distribution (Soltwisch, this conference). As a first step, the analysis code has been limited to circular plasmas with concentric flux surfaces $\psi(r)$. According to Callen and Dory (1972) this condition applies to plasmas with $\beta_p \ll 1$ (as was the case in TEXTOR). In addition, it is supposed that N_e is constant on a given flux surface and is thus only a function of the minor radius r . By contrast, the poloidal field B_{θ} varies like $1/R$ on a given surface (R being the major radius), causing the same $1/R$ -dependence for the Faraday rotation angles. The resulting relation between rotation angles to be measured in the inner and outer half of the plasma cross section provides a useful criterion to check the validity of the assumptions for practical applications. As a consequence of concentric flux surfaces, the current density distribution in the equatorial plane is asymmetric with its centre shifted towards the inner edge of the torus.

Figs. 4a-f give examples of phase shift and Faraday rotation measurements together with the results of the data analysis for a representative 300 kA discharge at 1 sec after start-up. In Fig. 4a the phase shifts are plotted versus the beam positions. The dots represent actual data points, whereas the crosses mark their mirror images relative to the plasma centre in order to demonstrate the symmetry of the phase shift profile. The curve is a spline fit to the data with some modification near the plasma edge. By inverting this profile the electron density distribution of Fig. 4b is obtained. The Faraday rotation angles are displayed in Fig. 4c together with a set of curves representing possible profiles compatible with the measurements. Each of them satisfies the assumption of concentric flux surfaces. Finally, Fig. 4d-f show the resulting horizontal distributions of poloidal field, safety factor, and current density. The spread of the curves gives an indication of the accuracy which rapidly decreases beyond $r/a = 0.7$. The edge values marked by dots in Figs. 4d,e are calculated from total plasma current and toroidal field and serve as an independent check on these results.

For the 500 kA discharges the observed Faraday rotation angles increased by about a factor of three, thus reducing the relative experimental errors. Figs. 5a,b show the time evolution of the electron and current density profiles for a shot with additional gas injection at constant rate as described in chapter 2 (in contrast to Fig. 4f, the current density distributions were calculated for a vertical plasma diameter to achieve symmetry with respect to $r = 0$). The sudden broadening of the electron density profile at 500 msec was probably due to the onset of strong gas injection. It was accompanied by a peaked current density distribution with a central value of about 250 Acm^{-2} corresponding to a safety factor of $q(0) = 0.73$. At the same time the inner interferometer channels detected distinct oscillations of the line-averaged electron density at a frequency of about 1.8 kHz. These oscillations were too fast to be observed in the Faraday rotation signals which had a time resolution of 3 msec. Subsequently the current density profile flattened and the oscillations disappeared. No efforts have been made so far to analyse the start-up phase of the discharge because of experimental

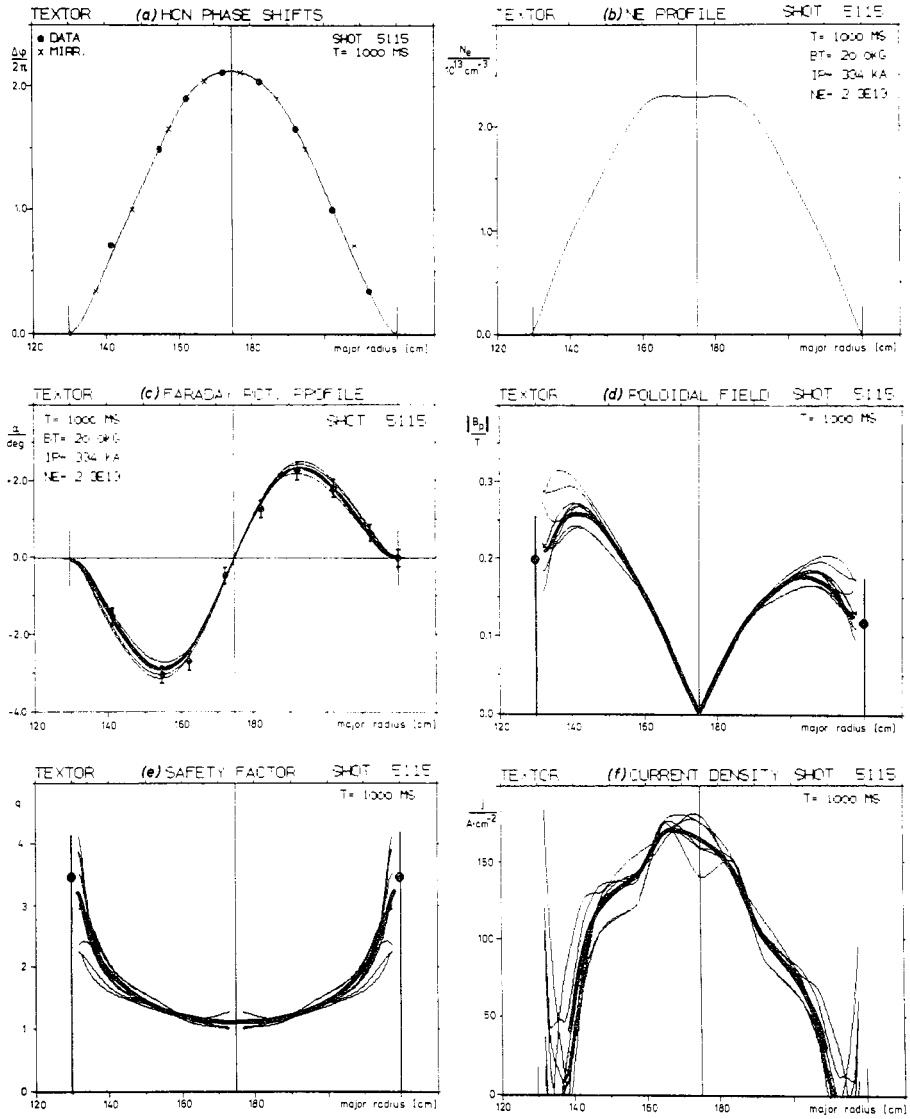


Fig. 4. Results of combined interferometric and polarimetric measurements obtained from a representative 300 kA discharge at 1 sec after start-up.

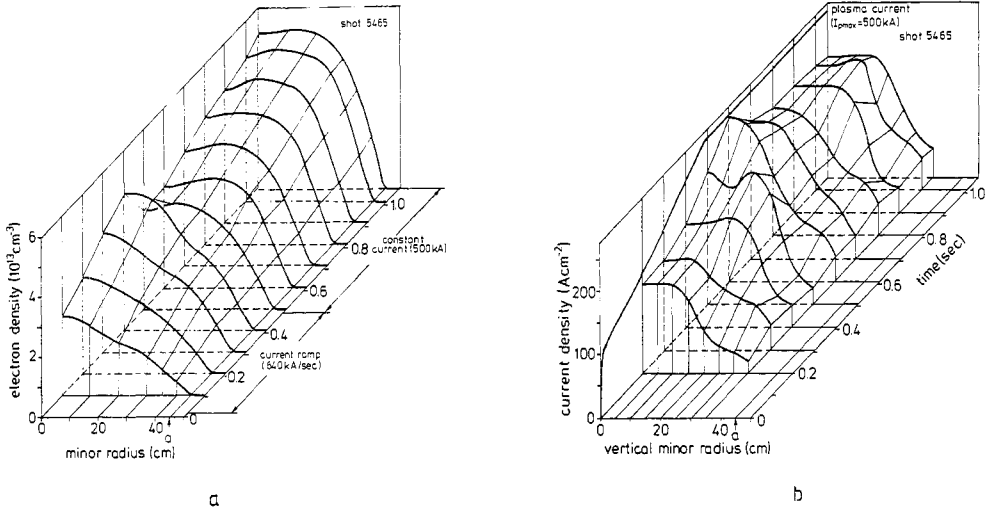


Fig. 5. Evolution of (a) the electron density profile and (b) the current density distribution for a 500 kA discharge with additional gas injection at constant rate during the current flat-top time.

difficulties during the fast current rise (mainly due to eddy current forces acting on some mirror mounts of the optical system).

6. NEUTRAL PARTICLE FLUXES FROM THE LIMITER AND IMPURITY CONCENTRATIONS IN THE PLASMA CORE

Most of the information on impurity concentrations was obtained from soft x-ray spectroscopy in the range from 0.8 to 8 keV. The instrument used was a pulse-height analyzer system comprising five spatial channels with 256 energy channels each. The spectra were registered in consecutive time intervals of 500 msec duration. From the line intensities the densities of the various impurity species were derived. The spectral shape of the continuum was used to determine the electron temperature. By normalizing the measured continuum to the bremsstrahlung continuum of hydrogen the enhancement factor was calculated to yield an estimate for the concentration of fully ionized low Z impurities (oxygen and carbon).

As a result for a well cleaned wall structure, the total concentration of metal impurities in the plasma centre was found to be 3×10^{-4} with an additional chlorine concentration of about 6×10^{-5} . The relative contributions of the metal species to this value roughly reflected the percentage composition of the limiter material, thus proving the limiters to be the dominant source of heavy impurities. The concentration of light impurities, inferred from the enhancement factor of the continuum, was less than 10^{-2} in satisfactory agreement with C VI and C V line intensities measured by VUV spectroscopy. With an upper limit of 10^{-2} for the oxygen concentration, the effective ion charge Z_{eff} in the plasma centre was less than 1.7. No impurity accumulation during prolonged discharge times was observed as demonstrated in Fig. 6, which shows a superposition of three soft x-ray spectra recorded in consecutive time intervals of 500 msec duration.

Neutral chromium and hydrogen fluxes from the limiters and ionization lengths of the released species were determined spectroscopically by observing the atomic line radiance near the limiter surface (Pospieszczyk *et al.*, this conference). The measurements took advantage of the fact that for typical densities $N_e \lesssim 10^{12} \text{ cm}^{-3}$ and temperatures $T_e \gtrsim 10 \text{ eV}$ the number of ionization processes and the atom fluxes are proportional to the number of photons emitted by the atoms (Equipe TFR, 1975). The layer surrounding the upper limiter was observed by means of a grating spectrometer whose entrance slit image touched the edge of the limiter and pointed towards the plasma centre (the main limiter configuration is schematically shown in Fig. 2). This positioning allowed to make spatially resolved measurements of the neutral particle distribution in the direction perpendicular to the limiter surface. In addition, the whole

poloidal cross section including the main limiters was observed in the light of neutral

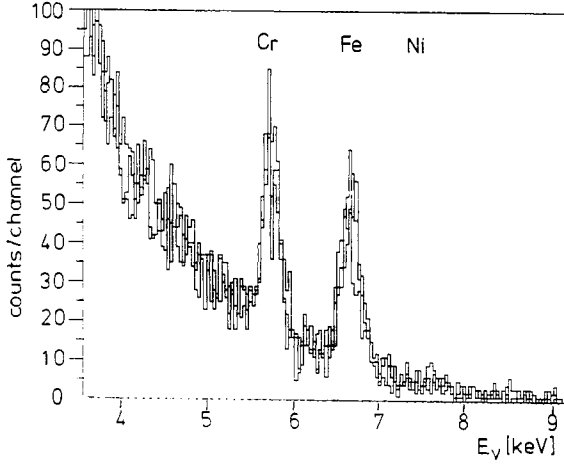


Fig. 6. Superposition of three soft x-ray spectra recorded in the time intervals 0.5-1.0 sec, 1.0-1.5 sec, 1.5-2.0 sec of a 300 kA discharge, showing no accumulation of Cr and Fe ions.

chromium or hydrogen by a CCD-camera system (charge coupled device with 488 x 380 picture elements; time resolution 20 msec) looking through appropriate interference filters.

The ionization length of metal impurities was estimated from the intensity decay away from the limiter surface. During the plateau phase of the discharges a typical length of 1 cm was found. With an electron temperature of 30 eV (confirmed by Thomson scattering) this value required an electron density of about $1 \times 10^{12} \text{ cm}^{-3}$ at the limiter. The spatial distribution of the H_{α} intensity was difficult to interpret due to a number of processes involved in its formation. From the spectral line shape it was concluded that the energy of hydrogen indeed rapidly values of more than 30 eV.

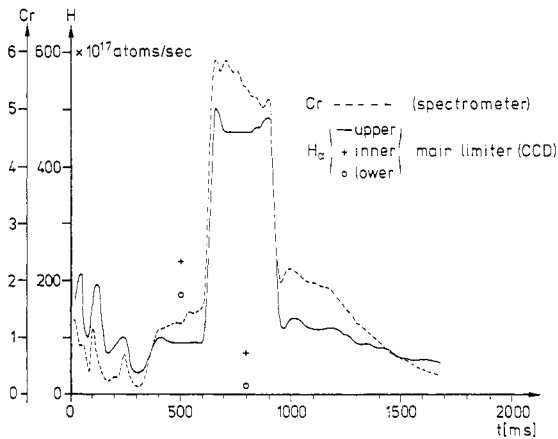


Fig. 7. Neutral chromium and hydrogen fluxes from the limiters (between 600 and 960 msec the plasma was shifted upwards).

Total particle fluxes from the Inconel limiters were derived from the absolute intensities of the spectral lines. The four segments of the main limiter gave a chromium flux of 6×10^{17} atoms/sec. Assuming equal sputtering yields for all constituents of Inconel and taking an impurity confinement time of 20 msec, this flux translates into an average metal concentration of 7×10^{-4} , which is in reasonable agreement with the soft x-ray measurements in the plasma core. The hydrogen atom flux from the limiters into the plasma, calculated from the H_{α} line intensity, was 6×10^{19} atoms/sec and thus only by a factor of 100 higher than the Cr flux. However, measurements of the hydrogen flux from the liner, taken at a toroidal position of 180° relative to the limiters, yielded a flux density of $2 \times 10^{15} \text{ cm}^{-2} \text{ sec}^{-1}$ and thus a total flux from the liner of 7×10^{20} atoms/sec. This value is a lower limit since the hydrogen flux density from liner areas near the limiter is usually enhanced. When the plasma was shifted towards the upper limiter, both the Cr and H fluxes increased up to a factor of four, whereas the fluxes from the other limiters decreased by a factor of about three (cf. Fig. 7). Obviously, the total released impurity flux remained about constant. Finally, it should be noted that the observed Cr flux cannot be explained by hydrogen sputtering but is most likely due to impurity ion sputtering.

Recently, the very sensitive technique of laser induced fluorescence (Bogen and Hintz, 1978) was applied to measure the iron density (and hence the flux) near the surface of a stainless steel test limiter positioned 1 cm outside the main limiter radius. Fig. 8 shows, as a preliminary result, the time evolution of the iron density detected with a temporal resolution of 10 msec. (Schweer and Bay, 1983)

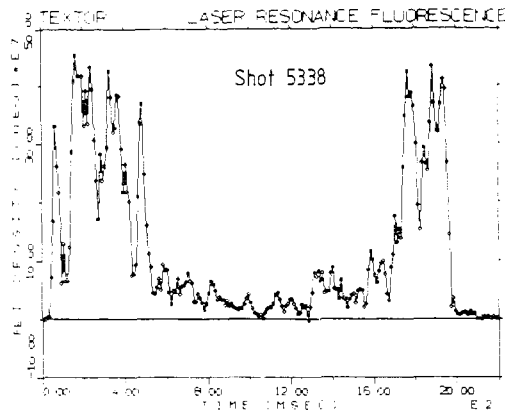


Fig. 8. Neutral iron density near the surface of a stainless steel test limiter positioned 1 cm outside the main limiter radius as detected by laser induced fluorescence.

7. LIMITER OBSERVATION BY MEANS OF INFRARED-THERMOGRAPHY

In order to evaluate the energy flux on to the limiters and to derive information on the scrape-off layer, the temperature distribution on the limiter surface was determined by infrared-thermography (Samm, this conference). For these measurements an additional half-sphere test limiter made of stainless steel was moved from below to the plasma boundary, and the main limiters were partly withdrawn. The thermal radiation emitted from the test limiter surface was observed simultaneously by a CCD-camera system (already mentioned in the previous chapter) and by a single PbSe element. The camera took a close-up view with a spatial resolution of 0.5 mm in both directions. It allowed to detect temperatures above 400°C with a dynamic range of 200°C and an accuracy of 3°C . For that reason the test limiter was preheated homogeneously to 400°C . The PbSe element could sense temperature excursions of more than 500°C with an error of 1°C and a time resolution of 100 μsec .

Fig. 9 is a typical infrared image of the test limiter with two clearly separated bright zones along the toroidal direction. Accordingly, a line scan of the corresponding video frame (Fig. 9c) showed almost no temperature rise on top of the limiter but two distinct

maxima on those parts of the surface which faced the plasma particle flow. Obviously, the heat flux was closely bound to the magnetic field lines. A detailed analysis of the temperature distribution, taking into account the spherical limiter geometry, yielded an exponential decay of the energy flux density in the limiter shadow with about the same energy scrape-off thickness of 1 cm for both the ion and electron sides (Fig. 9d). Care was taken to exclude the influence of the main limiters on the scrape-off layer by gradually withdrawing them behind the test limiter radius in a series of consecutive discharges. In addition, the plasma was shifted towards the test limiter for 0.8 sec during the flat-top time.

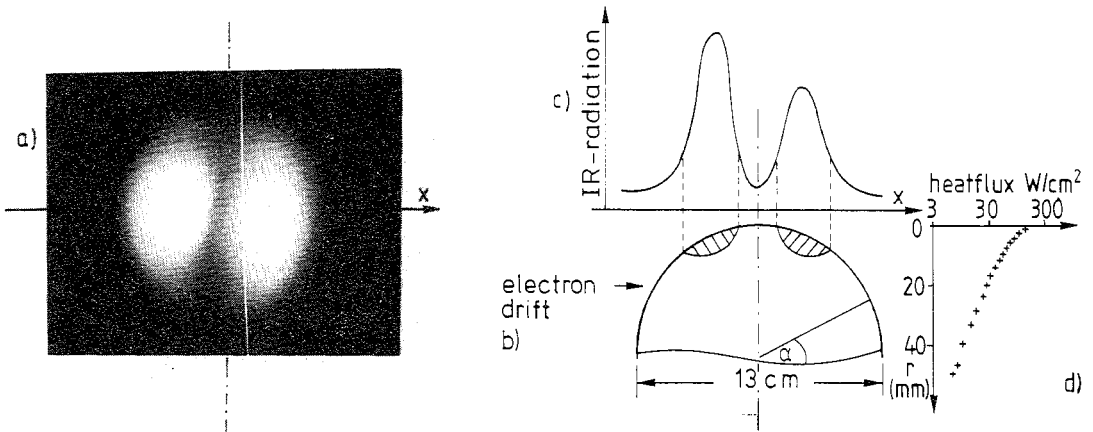


Fig. 9. (a) Typical infrared image of the test limiter, (b) side view of the test limiter, (c) line scan of the infrared signal, and (d) radial heat flux profile.

The absolute energy flux onto the limiter was determined from the temperature rise on the surface by adopting the simple model of constant heat flux to a semi-infinite uniform solid. This assumption was justified since the radius of curvature of the surface was large compared to the depth of temperature penetration. Furthermore, during the interval of plasma displacement the temperature was found to increase in proportion to the square root of time as expected for a constant heat flux. The power densities were measured at the point of maximum temperature and recalculated for the limiter top under consideration of the exponential decay. Depending on the position of the main limiters and on plasma shifts, values between 300 and 3500 Wcm^{-2} were derived. For standard discharges with well-centred plasmas and with test and main limiters set at the same radius, the average power density was 300 Wcm^{-2} yielding a total power load on to all limiter of 70 kW or about 15 % of the ohmic heating power input. This result was confirmed by calorimetric measurements obtained from thermocouples implemented in all limiter segments.

8. SUMMARY

The first six months of experimental work on TEXTOR were characterized by continuous progress in the generation and control of reproducible long-pulse plasmas as a prerequisite for forthcoming plasma-wall interaction research. The machine performance was steadily improved until it finally met the design goals for ohmic heating operation. The resulting plasmas (for a maximum plasma current of 500 kA, a toroidal field of 2 T and a liner temperature of 300 °C) had a life time of up to 2.2 sec, a maximum line-averaged density of $4 \times 10^{13} \text{ cm}^{-3}$ and a central electron temperature of about 1.2 keV. The metal impurities in the plasma centre had a concentration of only 3×10^{-4} and showed no accumulation during the pulse times. Discharges were maintained at a safety factor of $q(a) = 2.3$ for a flat-top time of 600 msec. TEXTOR provided high availability and dependable operation even at the lay-out limits.

Efficient control of the low Z impurities, as demonstrated by typical oxygen concentrations of less than 1 %, certainly had a substantial share in this performance. After a major opening of the vacuum vessel, a combination of RG discharge cleaning and baking brought the machine back to satisfactory operation in only a few days. Preliminary experiments with a thin carbon film on the first wall demonstrated the feasibility of simple plasma-chemical surface

modifications although their potential for the control of high Z impurities needs further verification.

Accurate centering of the plasma inside the limiter aperture was achieved by different techniques of position detection. In addition to standard magnetic diagnostics outside the liner, interferometric and polarimetric methods were employed. The latter are sensitive to plasma displacements rather than to motions and prevent even very slow drifts of the plasma column. Both techniques also proved to be fast enough to allow rapid pre-programmed shifts of the plasma and to handle sudden displacements caused by developing disruptions.

The pending task of measuring the current density distribution in Tokamak devices was tackled by utilizing the Faraday effect upon linearly polarized far-infrared radiation. An interpretation of the experimental results on the basis of concentric flux surfaces (which seemed justified by $\beta_p \ll 1$ and by experimental evidence) yielded reasonably accurate current density profiles for plasma radii $r/a \leq 0.7$. Refined methods of data analysis will be required for plasmas with strong additional heating and, consequently, eccentric flux surfaces.

First investigations in the field of plasma wall interaction - besides, of course, wall cleaning and conditioning - concentrated upon the limiters. By changing the material from Inconel to stainless steel, the limiters could be identified as the dominant source of metal impurities. Spectroscopic measurements of the neutral chromium flux strongly indicated that the metal atoms were mainly released by impurity ion sputtering. Concerning the neutral hydrogen flux from the liner and limiters, it was found that the liner gave the major contribution. For the electron density near the limiter surface a typical value of $1 \times 10^{12} \text{ cm}^{-3}$ was obtained. The total power load on to all limiters was determined by time resolved infrared-thermography, resulting in about 70 kW or 15 % of the ohmic heating input. Measurements of the temperature distribution on a test limiter surface showed an exponential decay of the power density in the limiter shadow with a scrape-off thickness of about 1 cm for both the ion and electron sides.

TEXTOR has been designed and built by the following team:

Physics: K.H. Dippel, H. Conrads, H. Gerhauser, A. Kaleck, H. Kever, P. Noll, A. Rogister, G. Waidmann, G. Wolf

Electrical Systems: B. Giesen, U. Braunsberger⁺, A. Brocke, M. Lochter, F. Petree⁺⁺, U. Pfister, W. Schalt, F. Schöngen, U. Schwarz, A. Seeger, E. Veiders.

Mechanical System: W. Kohlhaas, M. Schürer, C. Stickelmann, J. Vieth

Torus Vessels: D. Butzek

Vacuum System: K.H. Dippel, W. Bieger, H. Stechemesser, M. Schürer

Control and Data Acquisition: F.H. Bohn, H. Halling, W. Bertram, B. Görg, P.W. Hüttemann, M. Korten, K.H. Müller, F. Rongen, M. Sauer, W. Tenten, J. Zeumann

Instrumentation:
(Control/Diagnostics) G. Waidmann, A. Cosler, G. Fuchs, R. Kurz

Instrumentation:
(Safety) H. Lang, K. Matela, W. Wimmer

Projekt-Planning and Control: F.H. Bohn, H. Gresser

Head: H. Conrads

+ Institut für Hochspannungstechnik, TU Braunschweig
++ Ebasco Services, New York

The construction of TEXTOR has been significantly supported by:
Institut für Hochspannungstechnik der TU Braunschweig (Prof. Kärner, Prof. Salge)
Institut für technische Mechanik der RWTH Aachen (Prof. Rieder, Prof. Schomburg)

Institut für Statik und Dynamik der Luft- und Raumfahrtkonstruktion der Universität Stuttgart (Prof. Agyris)

During design and construction the continuous support and advice provided -within the frame of the IEA Implementing Agreement on TEXTOR between the European Community and the partners Canada, Japan, Switzerland, Turkey and USA- by several national laboratories, universities and companies were particularly valuable.

ACKNOWLEDGEMENTS

The authors would like to thank the members of the Institut für Plasmaphysik der KFA Jülich for their great efforts in assuring machine readiness and in operating the device.

The collaboration with the following institutes is gratefully acknowledged:

- A.F.I. Stockholm
- Institute for Physical and Chemical Research, Wako Shi,
- Institute for Plasmaphysics, Nagoya
- Japanese Atomic Energy Research Institute, Tokai Mura,
- Oak Ridge National Laboratory.

During construction as well as during operation TEXTOR has greatly benefitted by the firm backing and continuous engagement of the board of directors, KFA Jülich GmbH.

REFERENCES

- Bieger, W., Dippel, K.H., Fuchs, G., and G.H. Wolf (1976). Proc Int. Sym. on Plasma Wall Interaction, Pergamon, Oxford, pp. 609-618
- Bogen, P. and E. Hintz (1978) Comments Plasma Phys. Controlled Fusion, 4, 115-129
- Brocke, W.A., and G. Waidmann (1982). Proc. 12th Symp. on Fusion Technology, Vol.2, Pergamon Oxford, pp. 1179-1184.
- Callen, J.D., and R.A. Dory (1972). Phys. Fluids, 15, 1523-1528
- Conn, R.W., Froth, S.P., Prinjy, A.K., Gauster, W.B., Malinowski, M.E., Pontau, A.E., Blewer, R.S., Whitley, J.B., Dippel, K.H., and G. Fuchs (1982). Proc. 12th Symp. on Fusion Technology, Vol. 1, Pergamon, Oxford, pp. 497-504.
- Conrads, H. (1978). Proc. 10th Symp. on Fusion Technology, Vol 1, Pergamon, Oxford, pp.25-30.
- Equipe TFR (1975). Nucl. Fusion, 15, 1053-1066.
- Equipe TFR (1980). Nucl. Fusion, 20, 1227-1245.
- Gerhauser, H. (1978). Proc. 10th Symp. on Fusion Technology, Vol 2, Pergamon, Oxford, pp.951-955.
- Soltwisch, H. and Equipe TFR (1981). Infrared Phys., 21, 287-298.
- Soltwisch, H. (1983). to be published.
- Veron, D., Certain, J., and J.P. Crenn (1977). J. Opt. Soc. Am., 67, 964-967.
- Waelbroeck, F., Winter, J., Ali-Khan, I., Wienhold, P., Brandt, B., and K.J. Dietz (1980). Cleaning and Conditioning of the Walls of Plasma Devices by Glow Discharge in Hydrogen Report JÜL-1692, Kernforschungsanlage Jülich.
- Waelbroeck, F., Winter, J., Wienhold, P., Könen, L., Banno, T., Grobusch, L., Rota, E., Tschersich, K.G., and TEXTOR team (1983). Proc. 9th Intern. Vacuum Congress, Madrid.
- Waidmann, G. (1979). Interferometric Plasma Position Detection for Position Control in Tokamak Experiments, Report Jül-1579, Kernforschungsanlage Jülich
- Pospieszczyk, A., Bogen, P., and U. Samm (1983). Proc. 11th European Conf. Controlled Fusion and Plasma Physics, Vol.7 D, Eur. Phys. Soc., part II, pp.417-420.
- Samm, U. (1983). ibid., part II, pp. 413-416
- Soltwisch, H. (1983). ibid., part I, pp. 123-126.
- Waidmann, G. (1983). ibid., part I, pp. 103-106.
- Wienhold, P., Waelbroeck, F., Winter, J., Rota, E., and T. Banno (1983), ibid., part II, pp.393-396.
- Winter, J., Waelbroeck, F., Wienhold, P., Esser, H.G., Könen, L., Banno, T., and E. Rota (1983) ibid., part II, pp. 483-486
- Schweer, B., and H.L. Bay (1983). to be published.